

Bachelor's Degree Thesis

Enhanced χ -sepnet with Physics-Informed Unrolling:
Towards Accurate MRI Susceptibility Mapping

December 2023

College of Engineering, Seoul National University

Department of Electrical and Computer Engineering

Kang Wook Kim

Abstract

Quantitative Susceptibility Mapping (QSM) is an MRI technique that non-invasively maps the spatial distribution of susceptibility in biological tissues. QSM calculates the susceptibility by combining the effects of paramagnetic substances (e.g., iron) and diamagnetic substances (e.g., myelin) at each voxel. However, this approach has a limitation in that it cannot predict the individual distributions of iron and myelin separately.

To overcome this limitation, a method called χ -separation was developed, which separates and maps the distributions of paramagnetic and diamagnetic substances in the brain into χ_{pos} and χ_{neg} , respectively. A limitation of χ -separation is the requirement of multiple head orientation, which increases scan time and poses practical application challenges. Recently, Kim et al. introduced χ -sepnet, a neural network for estimating χ_{pos} and χ_{neg} maps from single head orientation data. χ -sepnet takes R'_2 and local phase maps obtained from single head orientation as inputs to estimate χ_{pos} and χ_{neg} maps.

In this paper, we present a method to improve the performance of χ -sepnet by enforcing physics through unrolling iterations. We represent the inputs, R'_2 maps and local phase maps, and the susceptibility map obtained from QSMnet, as a combination of outputs, χ_{pos} and χ_{neg} , and propose a model, Unrolled χ -sepnet- R'_2 , that enforces this relationship over multiple iterations. We evaluate Unrolled χ -sepnet- R'_2 on multi-echo GRE and multi-echo SE data from eight healthy subjects (divided into 4:1:3 for training, validation, and testing), and confirm that Unrolled χ -sepnet- R'_2 shows better metrics in NRMSE, PSNR, and SSIM than the baseline χ -sepnet- R'_2 . Additionally, we observe that the iteration-wise outputs of Unrolled χ -sepnet- R'_2 improve iteratively, demonstrating that the model increasingly predicts more accurate maps through iterations. Meanwhile, in Unrolled χ -sepnet- R'_2 , the underestimation phenomenon becomes more severe in simulated patient test data compared to the baseline, and further research needs to be conducted to resolve this.

Keywords : χ -separation, χ -sepnet, unrolling iteration, neural network

Table of Contents

Abstract	i
Table of Contents	ii
List of Tables	iii
List of Figures	iv
1 Introduction	1
2 Main Content	3
2.1 Backgrounds	3
2.1.1 χ -separation	3
2.1.2 χ -sepnet	3
2.2 Methods	4
2.3 Experiments	5
2.4 Results	5
2.4.1 Quantitative results	5
2.4.2 Qualitative results	6
2.4.3 Generalization to patient data	7
3 Conclusion	12
Bibliography	13

List of Tables

2.1 Comparative analysis of baseline and unrolled χ -sepnet performance: Quantitative evaluation of NRMSE, PSNR, and SSIM metrics for χ_{pos} maps (upper section) and χ_{neg} maps (lower section).	6
---	---

List of Figures

2.1	The overall architecture of our proposed model, Unrolled χ -sepnet- R'_2 . In this model, the input y is a concatenation of R'_2 , local phase, and susceptibility map. The neural network is represented by P_θ , which plays a crucial role in processing the input data. The relationship between the input and the output map is denoted by Φ , highlighting the model's ability to map these elements effectively. Additionally, α represents a learnable parameter within the network, emphasizing the adaptability and optimization of the model in learning from data.	5
2.2	Results across iterations for χ_{pos} (upper section) and χ_{neg} (lower section).	8
2.3	Error map across Iterations for χ_{pos} (upper section) and χ_{neg} (lower section).	9
2.4	Difference map from previous iteration for χ_{pos} (upper section) and χ_{neg} (lower section).	10
2.5	Unrolled χ -sepnet results for simulated hemorrhage cases (upper section) and simulated calcification cases (lower section).	11

Chapter 1

Introduction

Quantitative Susceptibility Mapping (QSM)[1] is an MRI technique that non-invasively maps the spatial distribution of susceptibility in biological tissue. QSM typically computes the susceptibility by combining the paramagnetic substances (e.g., iron) and diamagnetic substances (e.g., myelin) at each voxel. However, this computation has the limitation of not being able to separately predict the distribution of iron and myelin. As a result, while QSM provides useful insights, its utility is somewhat limited due to this constraint.

To overcome this limitation, a novel method called χ -separation[2] was developed. This method aims to separately map the distribution of paramagnetic and diamagnetic substances in the brain as χ_{pos} and χ_{neg} , respectively. However, χ -separation relies on multiple head orientation, significantly increasing scan time, thus posing challenges for practical applications. Recently, new approaches have been proposed to address this issue.

The approach proposed by Kim et al.[3] utilizes a neural network, χ -sepnet, which takes single head orientation data as input to predict χ_{pos} and χ_{neg} maps. This network processes the R'_2 and local phase maps obtained from single head orientation to estimate these distributions. This research suggests the practical applicability of this method by resolving the scan time issue of χ -separation. χ -sepnet is constructed with a U-net architecture, leaving room for potential improvements in the architecture.

In this paper, we apply an unrolling iteration technique to improve the output map accuracy of the χ -sepnet model. We leverage the physical principles that the input R'_2 and local phase maps and the susceptibility map obtained from QSMnet can be represented as a combination of χ_{pos} and χ_{neg} . This physical relationship is structurally reinforced through multiple iterations, thereby improving the accuracy of the output maps.

We evaluate this method using multi-echo GRE and multi-echo SE data from 8 healthy subjects (4:1:3 subjects for train:validation:test). As a result, we confirm that our model achieves better performance metrics, such as NRMSE, PSNR, and SSIM, compared to the baseline χ -sepnet- R'_2 .

The structure of this paper is as follows: Section 2.1 in Chapter 2 provides the background knowledge, including the physical relationship, followed by Section 2.2, where we present our model. In Section 2.3, we describe the experiments conducted to validate the model, and Section 2.4 interprets the results. Finally, Chapter 3 concludes the paper.

Chapter 2

Main Content

2.1 Backgrounds

2.1.1 χ -separation

χ -separation takes the local phase (Δf) and the R'_2 map obtained from multiple head orientations as input and estimates the χ_{pos} and χ_{neg} maps as output. According to previous studies [2], [4], the following physical relationship exists between these inputs and outputs:

$$\Delta f(\mathbf{r}) = D_f(\mathbf{r}) * (\chi_{\text{pos}}(\mathbf{r}) + \chi_{\text{neg}}(\mathbf{r})), \quad (2.1)$$

$$R'_2(\mathbf{r}) = D_{r,\text{pos}} \cdot |\chi_{\text{pos}}(\mathbf{r})| + D_{r,\text{neg}} \cdot |\chi_{\text{neg}}(\mathbf{r})|, \quad (2.2)$$

where D_f represents the dipole kernel for the dipole convolution operation, and D_r denotes a constant value. The values of D_r have been identified in previous studies [2]. However, since the dipole convolution operation in Equation 2.1 is non-invertible, the output cannot be directly calculated from the input. Regularization of the data obtained from multiple head orientation scanning is necessary to estimate the χ_{pos} and χ_{neg} maps.

2.1.2 χ -sepnet

Obtaining χ_{pos} and χ_{neg} maps from scanning via multiple head orientation is limited in practical use due to the excessively long scan time. Kim et al. [3] proposed χ -sepnet, a method that estimates the χ_{pos} and χ_{neg} maps using only the scanning data obtained from single head orientation. χ -sepnet receives the local phase and R'_2 maps as input and predicts the susceptibility (χ) map from the local phase through QSMnet [5]. The predicted susceptibility map is concatenated with the original two input maps and fed into the neural network to obtain the χ_{pos} and χ_{neg} maps. Additionally, Kim

et al. proposed a variant called χ -sepnet- R_2^* , which uses the R_2^* map, a relatively easier-to-obtain map during the scan process, instead of the R_2' map for prediction. While χ -sepnet- R_2^* has lower performance compared to χ -sepnet- R_2' , it is more practical for use.

2.2 Methods

Since the physical relationship between the input and output is known, we leverage unrolling iteration to enforce this knowledge within the model. Similar to χ -sepnet[2], we incorporate QSMnet[5] into our model’s process. Our model receives the local phase and R_2^* map along with the predicted susceptibility map as input. The susceptibility (χ) is expressed as the sum of χ_{pos} and χ_{neg} :

$$\chi = \chi_{\text{pos}}(\mathbf{r}) - \chi_{\text{neg}}(\mathbf{r}). \quad (2.3)$$

We enforce the physical relationships between the input and output in χ -separation as described by Equations 2.1, 2.2, and 2.3 through unrolling iteration. These relationships can be summarized as follows:

$$y = \Phi x + v, \quad (2.4)$$

where

$$y = \begin{bmatrix} \text{Sus} \\ R^2 \\ \Delta f \end{bmatrix}, \quad x = \begin{bmatrix} \chi_{\text{pos}} \\ \chi_{\text{neg}} \end{bmatrix}, \quad \Phi = \begin{bmatrix} I & -I \\ I & I \\ F^{-1}DF & -F^{-1}DF \end{bmatrix}, \quad v = \text{noise}.$$

Here, F and D represent the Fourier transform and dipole kernel, respectively.

The relationship between input y and output x is described by Equation 2.4, but since some of the equations are non-invertible, regularization is necessary to compute x from y . Given an arbitrary prediction \hat{x} for x , multiple iterations of minimizing $y - \Phi\hat{x}_i$ and regularizing this prediction \hat{x} can lead to a solution close to the true value of x . This process is known as unrolling iteration, and the procedure to predict \hat{x}_{i+1} from \hat{x}_i is described by the following equation:

$$\hat{x}_{i+1} = P_\theta (\alpha\Phi^H y + (I - \alpha\Phi^H\Phi)\hat{x}_i). \quad (2.5)$$

Here, P_θ represents the neural network, which regularizes x in the unrolling iteration. Additionally, α is a learnable parameter that is initialized to 4 based on previous studies[6], and its value is updated during training.

We propose a model that undergoes the iterative process of Equation 2.5 for a fixed number of iterations (10) and outputs the final prediction of χ_{pos} and χ_{neg} maps. We refer to this model as unrolled χ -sepnet- R_2' . The initial χ_{pos} and χ_{neg} maps are initialized to zero before the iteration begins. Figure 2.1 illustrates the overall structure of the unrolled χ -sepnet- R_2' model.

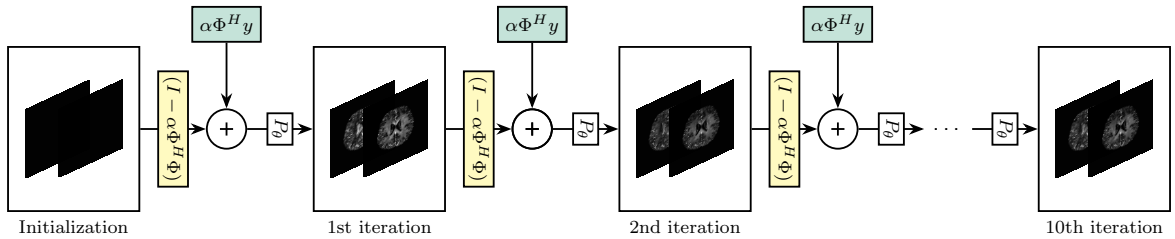


Figure 2.1: The overall architecture of our proposed model, Unrolled χ -sepnet- R'_2 . In this model, the input y is a concatenation of R'_2 , local phase, and susceptibility map. The neural network is represented by P_θ , which plays a crucial role in processing the input data. The relationship between the input and the output map is denoted by Φ , highlighting the model’s ability to map these elements effectively. Additionally, α represents a learnable parameter within the network, emphasizing the adaptability and optimization of the model in learning from data.

2.3 Experiments

The design of the proposed neural network is inspired by χ -sepnet[3], leading us to adopt a U-net architecture. Both in the training and inference phases, the final output is estimated through 10 iterations.

We evaluate our method by comparing the proposed model to the established χ -sepnet- R'_2 [3]. For this evaluation, we utilize multi-echo GRE and multi-echo SE data acquired from 8 healthy subjects (split as 4:1:3 for training: validation: testing). After training both our model and the baseline for 20 epochs on the training set, we test the models on the test set using the checkpoint with the lowest validation loss.

2.4 Results

In Section 2.4.1, we present the quantitative results, comparing PSNR and other metrics of our proposed model, Unrolled χ -sepnet- R'_2 , with the baseline. Section 2.4.2 presents the qualitative results, including susceptibility maps per iteration of the Unrolled χ -sepnet- R'_2 and empirical results.

2.4.1 Quantitative results

The results of the metrics measured on the test set are shown in Table 2.1. Compared to the baseline χ -sepnet- R'_2 [3], our proposed unrolled χ -sepnet- R'_2 demonstrates lower NRMSE and higher PSNR for both the χ_{pos} and χ_{neg} maps. In terms of SSIM, the baseline performs slightly better

χ_{pos}			
Method	NRMSE (\downarrow)	PSNR (\uparrow)	SSIM (\uparrow)
Baseline χ -sepnet- R'_2 [3]	33.72 ± 2.77	47.45 ± 0.94	0.94322 ± 0.00592
Unrolled χ -sepnet- R'_2	33.46 ± 2.83	47.52 ± 0.98	0.94307 ± 0.00600

χ_{neg}			
Method	NRMSE (\downarrow)	PSNR (\uparrow)	SSIM (\uparrow)
Baseline χ -sepnet- R'_2 [3]	35.79 ± 2.62	48.17 ± 0.70	0.94179 ± 0.00506
Unrolled χ -sepnet- R'_2	35.33 ± 2.72	48.28 ± 0.78	0.94246 ± 0.00536

Table 2.1: Comparative analysis of baseline and unrolled χ -sepnet performance: Quantitative evaluation of NRMSE, PSNR, and SSIM metrics for χ_{pos} maps (upper section) and χ_{neg} maps (lower section).

for the χ_{pos} map, but our unrolled χ -sepnet- R'_2 achieves a higher SSIM for the χ_{neg} map. Overall, our proposed unrolled χ -sepnet- R'_2 outperforms the baseline in terms of NRMSE, PSNR, and SSIM metrics, indicating that the output map quality of our model is superior.

2.4.2 Qualitative results

To verify that our iterative methods are functioning correctly and that the error decreases with each iteration, we present the error maps. Figure 2.2 shows the i -th prediction of the unrolled- χ -sepnet, while 2.3 displays the difference map between the i -th prediction and the ground truth label. As shown in Figure 2.3, the error between the prediction and the label decreases progressively with each iteration. Furthermore, Figure 2.2 reveals that during the initial iterations, alternating over-estimation and underestimation are observed. This indicates that our proposed unrolled- χ -sepnet produces more accurate output maps as iterations proceed. Additionally, Figure 2.4, which plots the difference between the i -th and $(i+1)$ -th predictions, shows that as the iterations continue, the changes between predictions become smaller, eventually stabilizing into a nearly unchanged iterative process in the later stages.

Furthermore, through conducting several ablation studies, we were able to empirically obtain various results:

- Increasing the number of iterations improves the metrics. However, this comes with a trade-off between memory usage and training/inference time.

- Excluding the use of the QSMnet map (susceptibility map) as input to the network results in a significant performance drop.
- Across various experimental settings, the value of α converges between 0.67 and 0.75.
- Regardless of changes in neural network architecture or modifications to α , the metric values eventually saturate at a certain level.
- When performing inference on patient data after training on healthy subjects, the Unrolled- χ -sepnet exhibits more severe underestimation compared to the existing baseline.

In particular, the underestimation becomes markedly more severe than the baseline, and this issue will be discussed in detail in the next subsection.

2.4.3 Generalization to patient data

In this experiment, we simulate patient cases by altering the χ_{pos} and χ_{neg} values of a specific brain region, obtained from a healthy subject, to fall within abnormal ranges, mimicking hemorrhage and calcification in that region. The resulting values from that region and the predicted values from the Unrolled χ -sepnet were plotted, and linear regression was performed on several data points, as shown in Figure 2.5. Since the neural network, acting as a regularization mechanism, has only seen normal data during training, it results in underestimation.

Both the Baseline and Unrolled χ -sepnet exhibit underestimation; however, a comparison of their slopes shows that the Unrolled χ -sepnet has a steeper decline. In other words, underestimation is more pronounced in the Unrolled χ -sepnet. This is hypothesized to occur because the Unrolled χ -sepnet passes through the neural network multiple times, compounding the underestimation. Evidence supporting this hypothesis includes experimental results showing that underestimation becomes more severe as the number of iterations increases. However, further research is required to fully validate this hypothesis. These results indicate that the Unrolled χ -sepnet generalizes worse to patient data compared to the baseline.

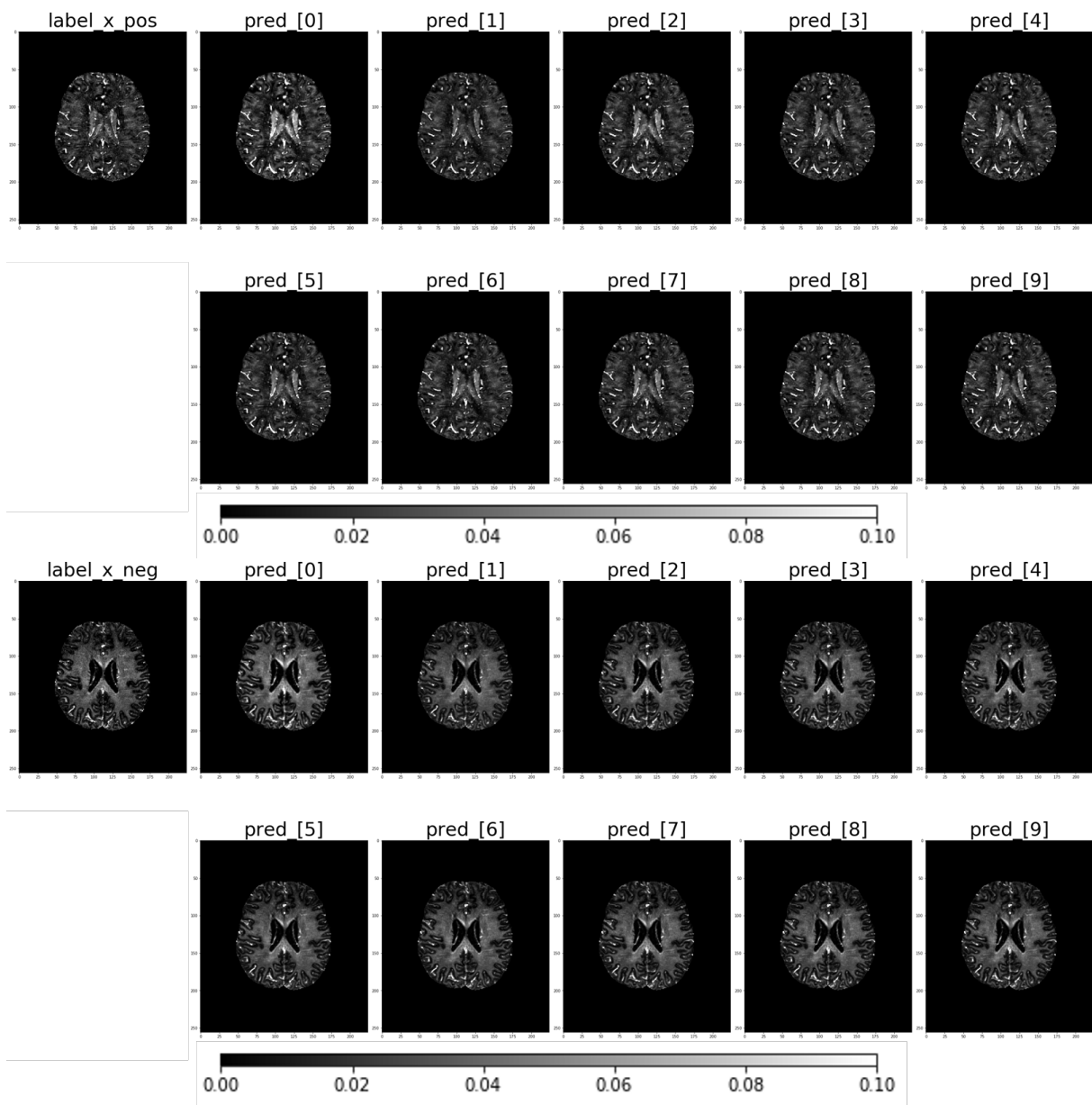


Figure 2.2: Results across iterations for χ_{pos} (upper section) and χ_{neg} (lower section).

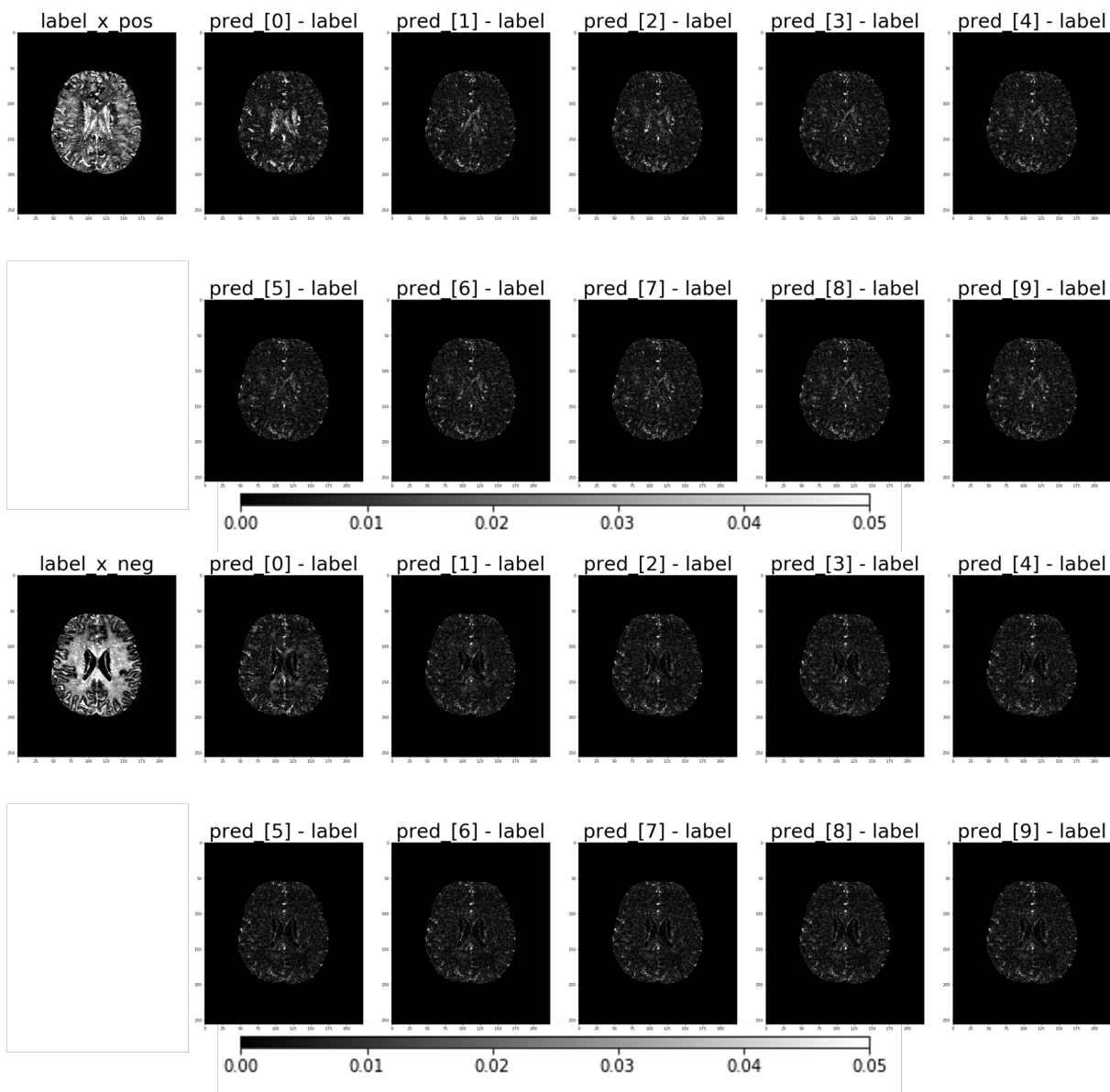


Figure 2.3: Error map across Iterations for χ_{pos} (upper section) and χ_{neg} (lower section).

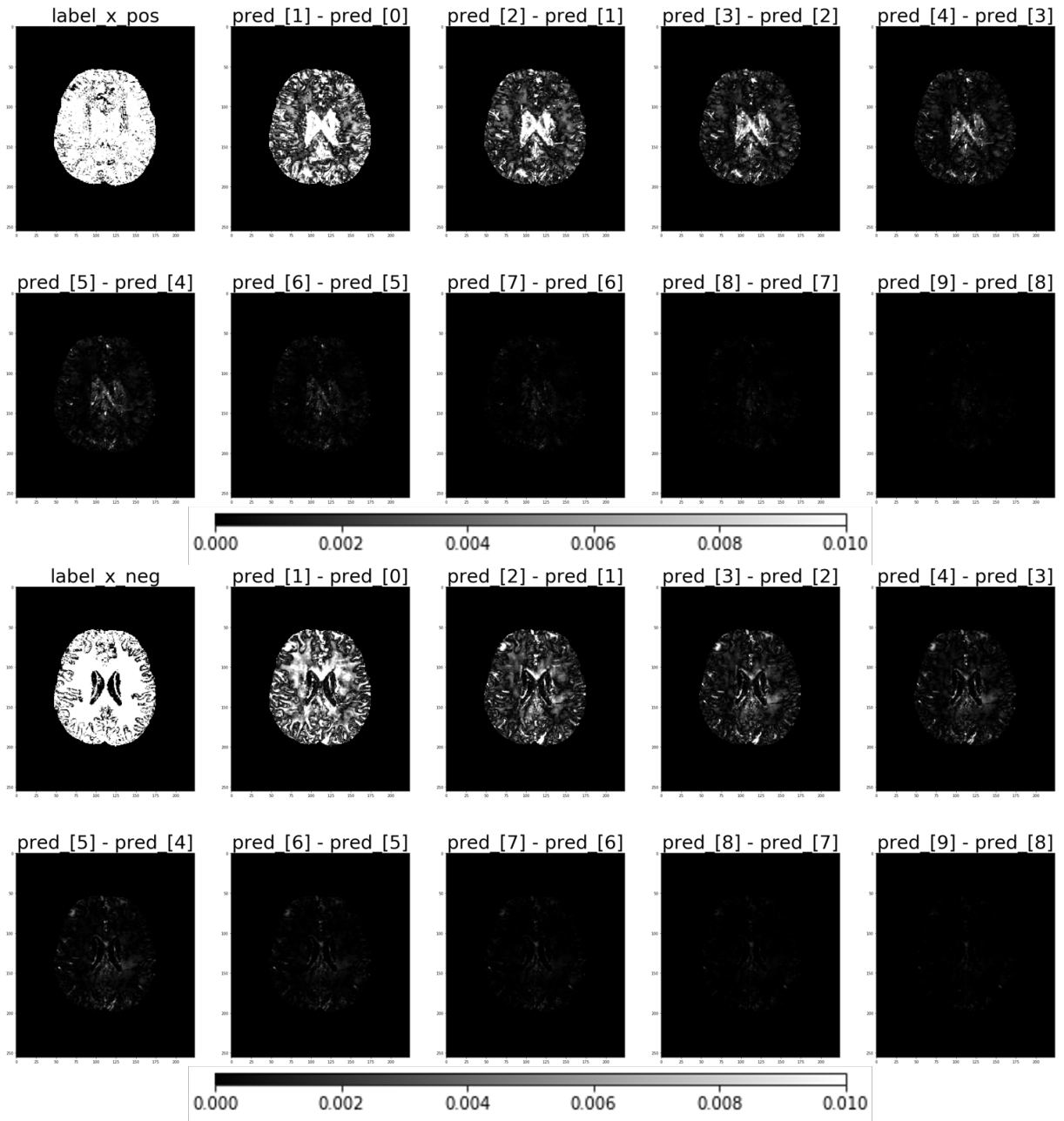
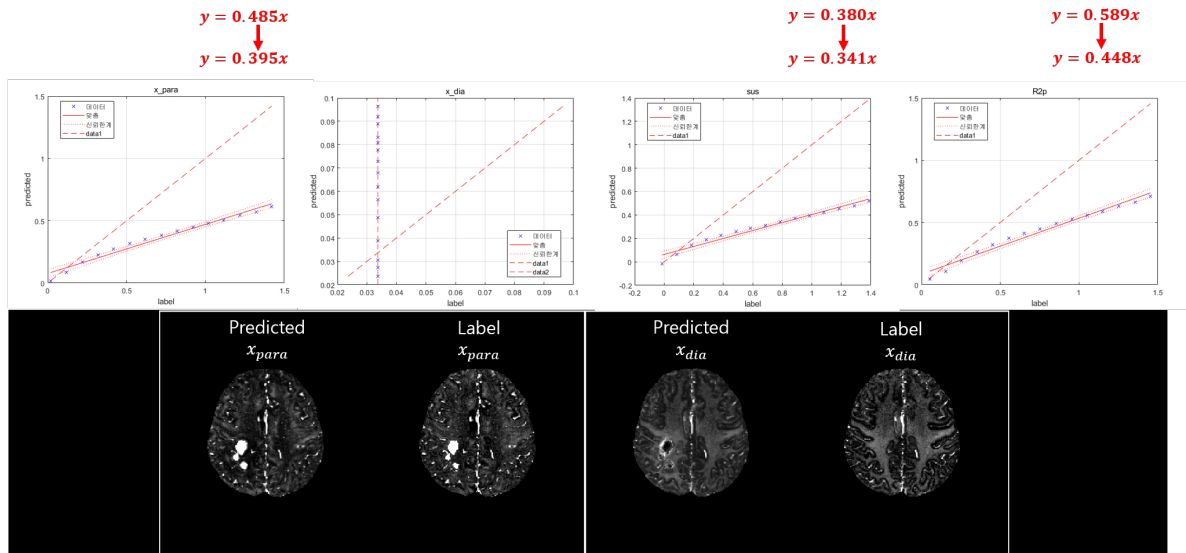


Figure 2.4: Difference map from previous iteration for χ_{pos} (upper section) and χ_{neg} (lower section).

Unrolled χ -sepnet- R_2' results

Simulated hemorrhage cases



Unrolled χ -sepnet- R_2' results

Simulated calcification cases

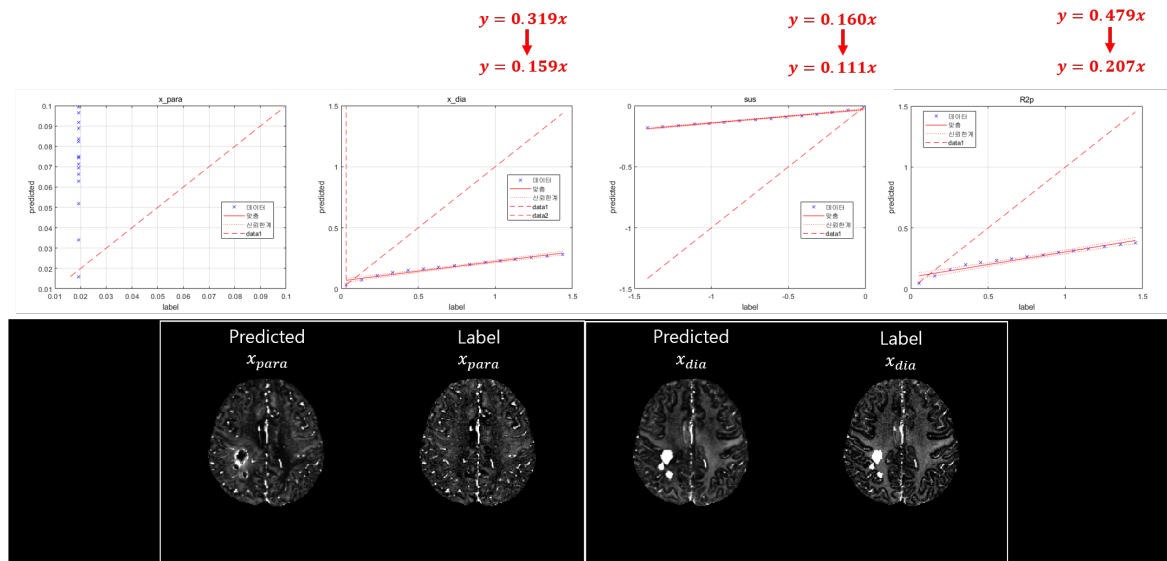


Figure 2.5: Unrolled χ -sepnet results for simulated hemorrhage cases (upper section) and simulated calcification cases (lower section).

Chapter 3

Conclusion

In this paper, we propose the Unrolled χ -sepnet as an improvement over the existing χ -sepnet. The Unrolled χ -sepnet enforces the physical relationship between the input (local phase, R'_2 map) and the output (χ_{pos} , χ_{neg} maps) across multiple unrolling iterations.

According to the results, Unrolled χ -sepnet- R'_2 demonstrated lower NRMSE and higher PSNR in the χ_{pos} and χ_{neg} maps compared to the Baseline χ -sepnet- R'_2 , and showed superior performance in the SSIM metric for the χ_{neg} map. This indicates that Unrolled χ -sepnet- R'_2 produces higher quality output maps than the baseline model.

Additionally, the effectiveness of iterative methods was confirmed through the error map, showing that the error decreases as the number of iterations increases. Initially, both overestimation and underestimation were observed alternately in the early iterations, but as the iterations progressed, the output maps of the Unrolled- χ -sepnet became increasingly accurate.

However, the Unrolled χ -sepnet showed inferior performance in generalizing to patient data compared to the baseline. Specifically, the underestimation phenomenon was more severe in the Unrolled χ -sepnet, which is hypothesized to result from compounding underestimation over multiple passes through the neural network. Further research is necessary to verify this hypothesis.

In summary, while the Unrolled χ -sepnet- R'_2 outperforms the baseline in specific metrics, improvements are still needed in terms of generalization to patient data.

Bibliography

- [1] C. Liu, H. Wei, N.-J. Gong, M. Cronin, R. Dibb, and K. Decker, “Quantitative susceptibility mapping: Contrast mechanisms and clinical applications,” *Tomography*, vol. 1, no. 1, pp. 3–17, 2015. DOI: 10.18383/j.tom.2015.00136. [Online]. Available: <https://doi.org/10.18383/j.tom.2015.00136>.
- [2] H.-G. Shin, J. Lee, Y. H. Yun, *et al.*, “ χ -separation: Magnetic susceptibility source separation toward iron and myelin mapping in the brain,” *NeuroImage*, vol. 240, p. 118371, 2021, ISSN: 1053-8119. DOI: <https://doi.org/10.1016/j.neuroimage.2021.118371>. [Online]. Available: <https://www.sciencedirect.com/science/article/pii/S1053811921006479>.
- [3] M. Kim, H.-G. Shin, C. Oh, *et al.*, “Chi-sepnet: Susceptibility source separation using deep neural network,”
- [4] R. Salomir, B. D. de Senneville, and C. T. Moonen, “A fast calculation method for magnetic field inhomogeneity due to an arbitrary distribution of bulk susceptibility,” *Concepts in Magnetic Resonance Part B: Magnetic Resonance Engineering*, vol. 19B, no. 1, pp. 26–34, 2003. DOI: <https://doi.org/10.1002/cmr.b.10083>. eprint: <https://onlinelibrary.wiley.com/doi/pdf/10.1002/cmr.b.10083>. [Online]. Available: <https://onlinelibrary.wiley.com/doi/abs/10.1002/cmr.b.10083>.
- [5] J. Yoon, E. Gong, I. Chatnuntawech, *et al.*, “Quantitative susceptibility mapping using deep neural network: Qsmnet,” *NeuroImage*, vol. 179, pp. 199–206, 2018, ISSN: 1053-8119. DOI: <https://doi.org/10.1016/j.neuroimage.2018.06.030>. [Online]. Available: <https://www.sciencedirect.com/science/article/pii/S1053811918305378>.
- [6] K.-W. Lai, M. Aggarwal, P. van Zijl, X. Li, and J. Sulam, “Learned proximal networks for quantitative susceptibility mapping,” in *Medical Image Computing and Computer Assisted Intervention – MICCAI 2020*, A. L. Martel, P. Abolmaesumi, D. Stoyanov, *et al.*, Eds., Cham: Springer International Publishing, 2020, pp. 125–135, ISBN: 978-3-030-59713-9.

Keywords: χ -separation, χ -sepnet, unrolling iteration, neural network